

Photo-production of axions in Supernovae

Sabyasachi Chakraborty,^{1,*} Aritra Gupta,^{2,†} and Miguel Vanvlasselaer^{3,‡}

¹*Department of Physics, Indian Institute of Technology, Kanpur-208016, India*

²*Instituto de Física Corpuscular (IFIC), CSIC, Parc Científic,
C/Catedrático José Beltrán, 2, E-46980 Paterna, Spain*

³*Theoretische Natuurkunde and IIHE/ELEM, Vrije Universiteit Brussel,
‡ The International Solvay Institutes, Pleinlaan 2, B-1050 Brussels, Belgium*

Compact stellar objects like supernovae and neutron stars are believed to cool by emitting axions predominantly via axion bremsstrahlung ($NN \rightarrow NNa$), pion conversion ($\pi^- p^+ \rightarrow Na$) and photo-production ($\gamma N \rightarrow Na$). In this paper, we study in detail the photo-production channel, from the unavoidable anomaly induced Wess-Zumino-Witten term $\propto \epsilon^{\mu\nu\alpha\beta} F_{\mu\nu} \partial_\alpha a \omega_\beta$ in conjunction with the low energy pion photo-production data. We found that for heavier axions, i.e., $m_a \sim \mathcal{O}(100)$ MeV, photo-production processes can be dominant compared to the usual axion emission processes. In addition, the spectrum of axions emitted in the process is significantly harder than those originating from bremsstrahlung.

I. INTRODUCTION

Searches for new physics much lighter than the electroweak scale have gained a lot of attention in the recent past. Among all the possible candidates, axions or axion-like particles are perhaps the most well-motivated. Axion emerges as the pseudo-Nambu-Goldstone boson of a spontaneously broken $U(1)$ symmetry [1–4] and offers a compelling solution to the long-standing strong- CP problem [5] of the Standard Model (SM). Moreover, axions can also be a natural dark matter candidate [6–8], address the hierarchy problem [9–11] and play a crucial role in resolving the matter-antimatter asymmetry [12, 13] of the Universe. Naturally, axion furnishes complementary means to probe physics beyond the SM at multiple frontiers.

While the axion can have a myriad of couplings with the SM particles, the most minimal effective Lagrangian addressing the strong CP problem, up to terms required for renormalization is given as:

$$\mathcal{L} = \mathcal{L}_{\text{SM}} + \frac{\alpha_s}{8\pi} \frac{a}{f_a} G\tilde{G} + \frac{1}{2} (\partial_\mu a)^2 - \frac{1}{2} m_{a_0}^2 a^2, \quad (1)$$

where G is the field strength tensor of the gluon and a is the axion with decay constant f_a . For lighter axions, $m_a \lesssim \mathcal{O}(\text{GeV})$, it is convenient to rotate away the $aG\tilde{G}$ coupling by a chiral transformation of the SM quark fields. The ensuing Lagrangian generates axion-quark kinetic and mass mixing terms and can be matched with an effective theory such as Chiral perturbation theory (χ PT) containing mesons. This effective description provides a powerful framework to study non-perturbative effects such as axion-pion mixing and has been used to constrain large parts of axion parameter space from intensity frontier experiments such as beam dump [14–16], rare decays

of pions [17–19] and kaons [20–27], etc. However, for heavy QCD axions, $m_a \gtrsim \mathcal{O}(1)$ GeV, the power counting of χ PT breaks down and one generally relies on perturbative computations to probe axions [28–31], mostly from rare B -decays.

On the other hand, the cosmic frontier provides complementary means to probe axions as it is sensitive to lighter masses, e.g., $m_a \lesssim \mathcal{O}(100)$ MeV. For example, nuclear reactions or thermal processes inside the stellar interior such as White Dwarf (WD), Neutron Star (NS), Supernova (SN), etc., are potentially powerful sources of axions. The emission of axions from such compact stellar objects might result in a more efficient transport of energy compared to the SM neutrinos, leading to observational changes. This lead the authors of Ref. [32, 33] to propose the following bound on the emissivity of axions

$$\frac{Q_a}{\rho} \lesssim 10^{19} \text{ erg s}^{-1} g^{-1}, \quad (2)$$

evaluated at a temperature $T = 30 - 50$ MeV and around the nuclear saturation density. Traditionally, axion bremsstrahlung, i.e., $NN \rightarrow NNa$ [34, 35], where $N = (p, n)$ is a nucleon, was considered to be the most dominant channel of axion production in the core of the SN. Although previous studies assumed One Pion Exchange (OPE) approximation, large suppression was found while going beyond OPE [36]. Nevertheless, using Eq.(2), earlier bounds were drawn on the axion mass and effective axion-nucleon coupling [37–43]. More recently, it was argued that pion conversion [44, 45] could potentially enhance the emissivity by a factor of few [46, 47], so is the existence of quark matter in the core of the SN [48]. We summarize those contributions and the relevant operators in Table I.

In this minimal scenario, it is natural to ask whether there exist any other unavoidable interactions of axions or not. For example, in the SM, there exists Wess-Zumino-Witten (WZW) interactions [51–60] which can account for certain processes including anomalies that can not be generated in the usual χ PT. This is because

* sabyac@iitk.ac.in

† aritra.gupta@ific.uv.es

‡ miguel.vanvlasselaer@vub.be

| Process | Coupling | Refs |
|---------------------------|---|-----------|
| $NN \rightarrow NN a$ | $(C_{aN}/2f_a) \bar{N} \gamma_5 \gamma_\mu N \partial^\mu a$ | [34, 35] |
| $\pi^- p \rightarrow N a$ | $(C_{aN}/2f_a) \bar{N} \gamma_5 \gamma_\mu N \partial^\mu a$ | [40, 46] |
| $N\gamma \rightarrow N a$ | $i (C_{aN\gamma}/2) a \bar{N} \gamma_5 \sigma_{\mu\nu} N F^{\mu\nu}$ | [49, 50] |
| $N\gamma \rightarrow N a$ | $(\kappa/f_a) \epsilon^{\mu\nu\rho\sigma} F_{\mu\nu} \partial_\rho a \omega_\sigma$ | This work |

TABLE I. Interactions relevant for axion emission from a supernova. The coefficient κ is defined in Eq. (6).

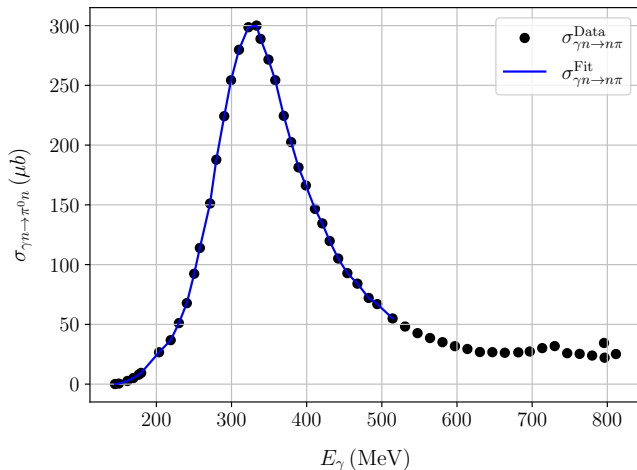


FIG. 1. Cross-section of the $\gamma p \rightarrow pa$ against the data from the PIONS@MAX-lab Collaboration [63] presented in [64–66]. In blue we present a fit on the data that we used for computing the emissivity.

low-energy effective theories such as χ PT can often possess more symmetries such as spurious parity than its UV counterpart QCD. Interestingly, in the presence of background gauge fields (such as ω , ρ mesons, etc.), the physics of WZW interactions are quite rich [58]. Recently it was shown that even in SM, such interactions open up new channels for the cooling of young neutron stars [57, 61, 62]. In this paper, we study the implications of photo-production $\gamma n \rightarrow na$ and WZW terms in the presence of axions leading to novel interactions. We also compare our process with the usual photo-production channels.

The paper is organized as follows. In section II we discuss in detail the different processes pertaining to axion photo-production. After briefly reviewing the widely used dipole operator, we point out the novel Wess-Zumino-Witten interaction which results in the photon initiated axion production in neutron rich stellar objects. We compute the emissivity for both degenerate and non-degenerate environments and found that this contribution is sub-leading compared to the usual processes. Finally, we also point out a complementary way of estimating the total emissivity from an entirely data-driven approach. Using low energy data of photon initiated pion production (see fig. 1), we estimate the overall axion

photo-production rate. Interestingly, this model independent study provides a comparable limit on the axion parameter space, for $m_a \sim \mathcal{O}(100)$ MeV. We also point out the hardness of the emitted axion spectrum and comment on its prospect of detection. Finally, in section III, we conclude.

II. PHOTO-PRODUCTION OF AXIONS

In this section, we provide a comparative study of the usual dipole induced axion photo-production channel with the novel WZW interaction and data driven approach.

A. Dipole induced photo-production:

Photo-production of axions can occur via the direct coupling of axions to nucleons and photons. This is usually induced through the unavoidable electric dipole portal, such as $i (C_{aN\gamma}/2) a \bar{N} \gamma_5 \sigma_{\mu\nu} N F^{\mu\nu}$. Implications of such an interaction have been studied in depth in [50], however, the bounds obtained on the axion decay constant are roughly around $f_a/\text{GeV} \gtrsim 6 \times 10^5$. This is indeed subleading compared to the prototypical axion cooling channels and even other photo-production processes stemming from the WZW and data driven contribution. As a consequence, we will neglect the possible cross terms between the other channels and the electric dipole that could arise. Nevertheless, dipole induced interactions can have interesting signatures in future neutrino experiments.

B. Wess-Zumino-Witten induced photo-production:

To generate WZW interactions, one considers the 5-dimensional action [51, 52] which is invariant under chiral symmetry, where the boundary is identified with our 4-dimensional spacetime, e.g.,

$$S_{\text{WZW}}(A_\mu, U) = N_c \int_D d^5 y \omega, \quad (3)$$

$$\omega = -\frac{i}{240\pi^2} \epsilon^{\mu\nu\rho\sigma\tau} \text{Tr}(\mathcal{U}_\mu \mathcal{U}_\nu \mathcal{U}_\rho \mathcal{U}_\sigma \mathcal{U}_\tau).$$

Here $\mathcal{U} = U^\dagger \partial_\mu U$ with $U = \text{Exp}(2i\pi^a T^a / f_\pi)$. π_a are the pion fields with decay constant f_π and A_μ 's are the gauge fields. The coefficient $N_c = 3$ is fixed by matching with QCD. Any arbitrary subgroup of the chiral symmetry can be gauged but only in the 4-dimension using the trial and error method. The full result has been nicely tabulated in [52] (also see [51, 53–56]). Meson fields such as ω can be introduced as a background vector field as prescribed in Ref. [57] by replacing $\hat{A}_\mu = A_\mu + B_\mu$ in the effective action. If the fundamental gauge fields are vector-like,

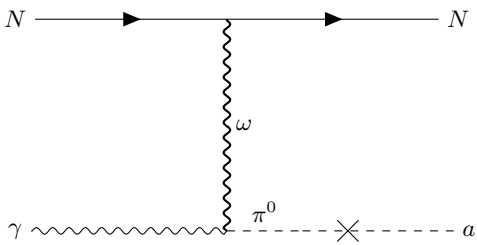


FIG. 2. Cooling of supernovae and neutron stars via $N\gamma \rightarrow Na$ induced by axion-WZW interactions. The cross indicates pion-axion mixing.

i.e., $A_L = A_R$, one needs to add appropriate counter-terms to maintain gauge invariance and conservation of vector current. Finally, tracking interactions with the pion fields (see Appendix A for details), we find

$$\mathcal{L}_{WZW}^{\pi^0} \supset \frac{N_c}{24\pi^2} \epsilon^{\mu\nu\rho\sigma} F_{\mu\nu} \left[\frac{e^2}{4} \frac{\pi_0}{f_\pi} F_{\rho\sigma} + eg_\omega \frac{\partial_\rho \pi_0}{f_\pi} \omega_\sigma \right]. \quad (4)$$

Starting from Eq. (1), axions can be incorporated in this framework by a suitable chiral transformation on the SM quark fields. This generates a mass-mixing between the axion and pion fields (shown by a cross in Fig. (2)). The mixing angle can be approximated as [67–69]

$$\theta_{\pi^0-a} \simeq \frac{f_\pi}{2f_a} \left(\frac{m_d - m_u}{m_u + m_d} \right) \equiv \frac{f_\pi}{f_a} C_A. \quad (5)$$

We then trade the mixing angle between axion and pion fields, which generates axion-photon coupling and the desired interactions of the form

$$\mathcal{L}_{WZW}^a \supset \frac{\kappa}{f_a} \epsilon^{\mu\nu\rho\sigma} F_{\mu\nu} \partial_\rho a \omega_\sigma, \quad \kappa = \frac{C_A N_c}{24\pi^2} eg_\omega. \quad (6)$$

On the other hand, nucleons interact with the vector meson fields ω via

$$\mathcal{L}_0 = \bar{N} (i\not{\partial} - g_\omega \not{\omega} - m_N) N, \quad (7)$$

where g_ω is estimated using nuclear physics and its value depends on the fitting model at hand. It is however estimated to be roughly $g_\omega \approx 10 - 12$ [70]. More generally, from the total cross-section for the pion production, we can obtain the rate for the axion production

$$\sigma_{\gamma n \rightarrow na} = \theta_{\pi^0-a}^2 \sigma_{\gamma n \rightarrow n\pi^0}, \quad (8)$$

in the regime $E \gg m_a, m_\pi$.

1. Computing the emissivity

As depicted in Fig. 2, Eq. (6) and Eq. (7) provide an efficient production channel of axions in a nucleon rich environment. The coupling f_a , dictates whether the axions can come out of the stellar object or get trapped inside it.

In the former case, axions can carry a part of the internal energy of the core with them, resulting in the cooling of the star. To estimate, we compute the emissivity Q , defined as the emitted energy per unit volume and per unit time. We take into account both neutron degenerate (D) as well as non-degenerate (ND) scenarios, mimicking the situation inside an NS and SN respectively. The emissivity for axion photo-production $\gamma N \rightarrow Na$ is given by

$$Q_{N\gamma \rightarrow Na} \equiv \int \frac{d^3 \vec{p}_\gamma f_\gamma(p_\gamma)}{(2\pi)^3 2E_\gamma} \int \frac{d^3 \vec{p}_{N_1}}{(2\pi)^3 2E_{N_1}} \frac{d^3 \vec{p}_{N_2}}{(2\pi)^3 2E_{N_2}} g_\gamma g_N \int \frac{d^3 \vec{p}_a}{(2\pi)^3 2E_a} E_a \langle |\mathcal{M}|^2 \rangle f_N(E_{N_1}) (1 - f_N(E_{N_2})) \times (2\pi)^4 \delta(E_{N_1} - E_{N_2} - Q_0) \delta^3(\vec{p}_{N_1} - \vec{p}_{N_2} - \vec{q}), \quad (9)$$

$$\approx \int \frac{g_\gamma d^3 \vec{p}_\gamma}{(2\pi)^3} f_\gamma(p_\gamma) \int \frac{g_N d^3 \vec{p}_N}{(2\pi)^3} f_N \sigma_{\gamma N \rightarrow Na}(E_\gamma) E_a,$$

where $\sigma(E_\gamma)$ is the integrated cross section. where $g_{\gamma(N)} = 2$ are the dof. of the photon (neutron), f_N is the neutron distribution function, E_i and \vec{p}_i are the energies and three-momenta of the i^{th} species and $Q_0 \equiv E_a - E_\gamma$, $\vec{q} \equiv \vec{p}_a - \vec{p}_\gamma$. The kinematics of the process is similar to a fixed target experiment where the initial neutron is assumed to be at rest. Due to the momentum transfer, the final neutron receives a kick and we consider them to be nearly non-relativistic thereby expanding their energies as $E_{N_i} \approx m_N + \mathcal{O}(\vec{p}_{N_i}^2/2m_N)$. The nucleon density is given by

$$n_B \equiv \int \frac{d^3 p_N}{(2\pi)^3} g_N f_N, \quad n_B = 4.5 \times 10^6 \rho_{15} \text{ MeV}^3.$$

Thus the emissivity from photo-production finally simplifies to

$$Q_{N\gamma \rightarrow Na} \approx \int \frac{dE_\gamma}{\pi^2} E_\gamma^3 f_\gamma(p_\gamma) n_B \sigma_{\gamma N \rightarrow Na}(E_\gamma), \quad (10)$$

We now turn to the computation of the emissivity using Eq.(10).

2. Emissivity from WZW term alone

We first compute the emissivity from the WZW term only. The spin averaged cross section reads

$$\sigma^{\text{WZW}}(E_\gamma) \approx \frac{1}{3\pi} \frac{\kappa^2 g_\omega^2}{f_a^2 m_\omega^4} \sqrt{1 - \frac{m_a^2}{E_\gamma^2}} E_\gamma^2 (E_\gamma^2 - m_a^2). \quad (11)$$

Here, θ is the angle between the axion and photon three momenta. The kinematics of the process dictates $E_a \sim E_\gamma$ when $m_\gamma \ll T$. This is a reasonable approximation as in the core of SN, the photons acquire a mass of the order of $m_\gamma \sim \mathcal{O}(10) \text{ MeV} \times (Y_e \rho_{14})^{1/3}$, where Y_e is the electron fraction. Since $T/m_\gamma \sim (3-4)$, we therefore do not expect the mass of the photon to play a significant role.

3. Non-degenerate scenario

For ND neutrons, the absence of Pauli blocking helps us to further simplify Eq. (10) as $1 - f_N(p_N) \approx 1$. Using the thermal distribution for photons [71] and integrating the axion energy from (m_a, ∞) , we find

$$Q_{N\gamma \rightarrow Na}^{\text{WZW,ND}} \approx g_\gamma g_\omega^2 \frac{\kappa^2 n_b}{2\pi^3} \frac{T^2}{f_a^2} \frac{m_a^4}{m_\omega^4} \left[4m_a T K_3 \left(\frac{m_a}{T} \right) + (m_a^2 + 35T^2) K_4 \left(\frac{m_a}{T} \right) \right], \quad (12)$$

where $K_{3,4}$ are the Bessel function of type three and four respectively. In the limit of $m_a \rightarrow 0$, the expression in Eq.(12) further simplifies to

$$\frac{Q_{\gamma N \rightarrow Na}^{\text{WZW,ND}}}{10^{32} \text{ erg/s/cm}^3} \approx 2.2 g_{10}^4 T_{40}^8 \rho_{15} \left(\frac{C_A 10^9}{f_a/\text{GeV}} \right)^2, \quad (13)$$

here we define T_{40} as $(T/40 \text{ MeV})$ and $g_{10} \equiv (g_\omega/10)$. The temperature dependence in Eq. (13) can be understood as the phase space scales as T^3 , the cross-section and emitted energy as T^4 and T respectively.

4. Degenerate scenario

The derivation of the cooling rate is more involved when neutrons are degenerate inside a medium. We closely follow the derivation of Ref. [61] (see also Appendix B) to write the emissivity in terms of the momentum transfer and obtain,

$$\frac{Q_{\gamma N \rightarrow Na}^{\text{WZW,D}}}{10^{32} \text{ erg/s/cm}^3} \approx 0.66 g_{10}^4 T_{40}^9 \left(\frac{C_A 10^9}{f_a/\text{GeV}} \right)^2. \quad (14)$$

The final emissivity is given by the minimum of the degenerate and the non-degenerate expressions: $Q^{\text{WZW}} = \text{Min}[Q_{\text{D}}^{\text{WZW}}, Q_{\text{ND}}^{\text{WZW}}]$. At the saturation density $\rho \sim \rho_0 \approx 0.3 \times 10^{15} \text{ g cm}^{-3}$, we obtain that the rate is

$$Q^{N\gamma \rightarrow Na} = \begin{cases} Q_{\text{D}}^{N\gamma \rightarrow Na} & T \lesssim 40 \text{ MeV} \\ Q_{\text{ND}}^{N\gamma \rightarrow Na} & T \gtrsim 40 \text{ MeV} \end{cases} \quad (15)$$

and we conclude that for the SN, it suffices to use the ND limit. On Fig. 3, we show the emissivity of the photo-production and compare it with pion conversion and bremsstrahlung.

At this point, it is worth mentioning that the high densities in the SN cores lead to the modification of the masses and the couplings. In Appendix C, we find a very modest in medium uncertainties

$$\frac{Q_{N\gamma \rightarrow Na}^*}{Q_{N\gamma \rightarrow Na}} \approx \frac{m_\omega^4}{g_\omega^4} \frac{g_{\omega^*}^4}{m_{\omega^*}^4} \in [0.8, 1.5]. \quad (16)$$

From those considerations, it is clear that cooling from the WZW term is subdominant by at least an order

of magnitude compared to the prototypical processes as shown in Eq. (2). Although the result strongly depends on the effective coupling g_ω , we note that it is constrained by nucleon phase-shift and photon-proton scattering data¹. Therefore, in this work, we consider it to be $g_\omega \sim g_\pi$.

C. Data-driven approach of axion photo-production

In this section, we take a complementary approach and propose a data-driven way of probing the axion parameter space. Recently the PIONS@MAX-lab Collaboration [63] measured the total photo-production cross-section of pions near the threshold. The collected data of $p\gamma \rightarrow p\pi_0$ in the region $E_\gamma = 145 - 180 \text{ MeV}$ [64] fits well with the predictions from SAID MA19 [65] and MAID2007 [66].

Similarly, the A2 collaboration at MAMI reported a new and precise determination of the differential and total cross section for $p\gamma \rightarrow p\pi_0$ in the energy range $E_\gamma = 180 - 500$ [72]. We fit the pion photo-production cross section using these data points, as shown in Fig.1. This, in turn, allows us to determine the axion photo-production cross-section, i.e., $\sigma_{\gamma N \rightarrow Na}$ in an entirely data-driven way. Integrating from threshold $E_\gamma \in [145, 500] \text{ MeV}$, we obtain a characteristic fit for the axion emissivity as

$$\frac{Q_{\text{data}}}{10^{33} \text{ cm}^{-3} \text{ s}^{-1} \text{ erg}} \approx 1.54 \left(\frac{C_A 10^9}{f_a/\text{GeV}} \right)^2 \rho_{15} T_{40}^{6.73}, \quad (17)$$

where the exponent of the temperature 6.73 provides a good fit to the numerical evaluation with χ^2 of 0.6 for Temperatures $T \in [30, 50] \text{ MeV}$ and is presented in Fig.3. Clearly, the data-driven contribution to axion emissivity dominates over the WZW term. In the regime where data is not present, i.e., $E_a \in [0, m_\pi]$, we compute the emissivity via the WZW term alone. This emissivity is compared with other sources of axions during SN in Fig.3.

D. Additional suppressing effects:

We now discuss the inclusion of subtleties that might modify the cooling computation, namely, the absorption in the core and the lapse effect.

1. Absorption and decay inside the SN core

The cooling argument in Eq. (2) applies only when the axions can free-stream through the SN core and do not

¹ We thank Andrea Caputo for pointing those available data to us.

get trapped[38]. Absorption proceeds via $aN \rightarrow \gamma N$ and $NNa \rightarrow NN$, [73–75]. For the mean free paths we obtain

$$\frac{L_a^{pn \rightarrow \gamma pn}}{10 \text{ Km}} \approx \frac{10^2}{X_p C_{ap}^2} \left(\frac{f_a}{10^9 \text{ GeV}} \right)^2 \frac{E_a}{1 \text{ GeV}}, \quad (18)$$

and

$$\frac{L_a^{N \rightarrow N\gamma}}{10 \text{ Km}} \approx \frac{\rho_{15}^{-1}}{C_A^2} \frac{250}{g_{10}^4} \left(\frac{f_a}{10^9 \text{ GeV}} \right)^2 \left(\frac{1 \text{ GeV}}{E_a} \right)^4. \quad (19)$$

This translates into a lower and an upper bound on the energy of the escaping axion. Therefore, Eq. (12) was an estimate based only on free-streaming axions. We impose these cut-offs on the axion energy while deriving the final limits on the axion parameter space, shown on Fig. 4.

Moreover, if the axion is massive, it can decay to two photons due to the unavoidable coupling $\mathcal{L} \subset G_{a\gamma\gamma} a \vec{E} \cdot \vec{B}$. The rate for this decay is [76]

$$\begin{aligned} L_{a \rightarrow \gamma\gamma} &= \frac{64\pi}{G_{a\gamma\gamma}^2} \frac{\sqrt{E_a^2 - m_a^2}}{E_a^4} \\ &\approx \frac{4 \times 10^4 \text{ km}}{(G_{a\gamma\gamma}/10^{-9} \text{ GeV}^{-1})^2} \frac{E_a/100 \text{ MeV}}{(m_a/100 \text{ MeV})^4}. \end{aligned} \quad (20)$$

Since $G_{a\gamma\gamma} \sim 1/(4\pi f_a)$ (which is generated at loop level in our minimal model), we conclude that for $f_a \gtrsim 10^7$ GeV and $m_a < 300$ MeV, the axion is always stable on the scale of the core. We will not consider this possibility anymore.

2. Lapse effects

The proto-neutron star is a very dense environment and gravitational effect will impact the emissivity via mostly two mechanisms:

1. The overall energy of the emitted axions is red-shifted,
2. Heavy axions will be trapped[74, 75, 77].

To account for this effect, we introduce a lapse factor $\alpha(M, r) \simeq \sqrt{1 - 2M/r^2}$, and the emissivity gets modified to[76]

$$Q_{N\gamma \rightarrow Na}^{\text{lapse effects}} \approx \int_{\frac{m_a}{\alpha}} \frac{dE_\gamma}{\pi^2} E_\gamma^3 f_\gamma(p_\gamma) n_B \sigma \times \alpha^2, \quad (21)$$

where $\alpha \equiv \alpha(M_{\text{SN}}, R_{\text{SN}})$. For $R_{\text{SN}} = 10$ km and $M_{\text{SN}} = M_{\text{sun}}$, $\alpha \approx 0.84$.

² We caution the reader that this expression neglects contributions from the pressure and energy of the stellar medium.

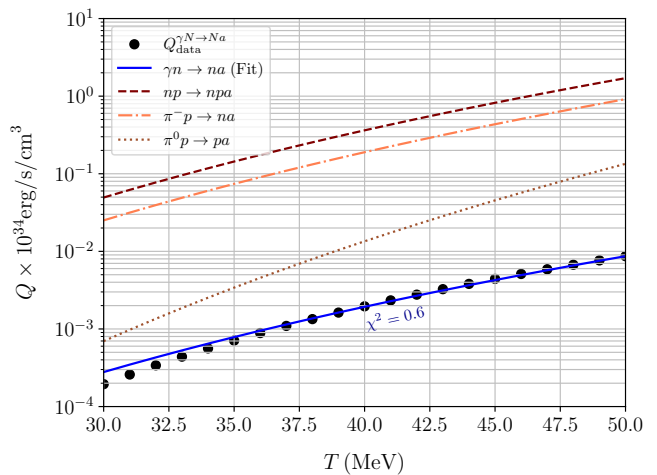


FIG. 3. Comparison of the emissivity rates from axion bremsstrahlung and pion conversion from [47, 78] with WZW photo-production (blue line). The black dot points are the numerical estimates of the emissivity integral, while the blue line is the fit presented in Eq.(17). For photo-production, we find that the data-driven approach contributes dominantly.

E. Implications of the photo-production

We summarize our results in fig. 4 where we show that photo-production alone can exclude regions, if $m_a \lesssim 100$, with $f_a \lesssim (0.4, 1) \times 10^8$ GeV for $T \sim (35, 45)$ MeV respectively. This is however subleading to the previous constraints, deduced from simulations in[75], which reaches $f_a \lesssim 0.77 \times 10^9$ GeV for $m_a \lesssim 50$ MeV in most of the parameter space. The trapping region beyond $f_a \lesssim 10^7$ can in principle be probed through detailed simulations including both the WZW and the bremsstrahlung type of interaction, however, it is beyond the scope of our present analysis. We also attract attention to the corner of large m_a axions, which might exceed the previous bounds. Even if they have been introduced in a phenomenological way in this study, a more complete inclusion of lapse effects and decay of the axion in flight might influence this conclusion and would need further numerical investigation.

It is also important to mention that the landscape of QCD axion models is quite broad. Without going into the details of such different scenarios, we consider a minimal situation given by Eq. (1), similar to the KSVZ [85, 86] framework. However, we find that similar conclusions hold in other types of axion models such as DFSZ [87, 88].

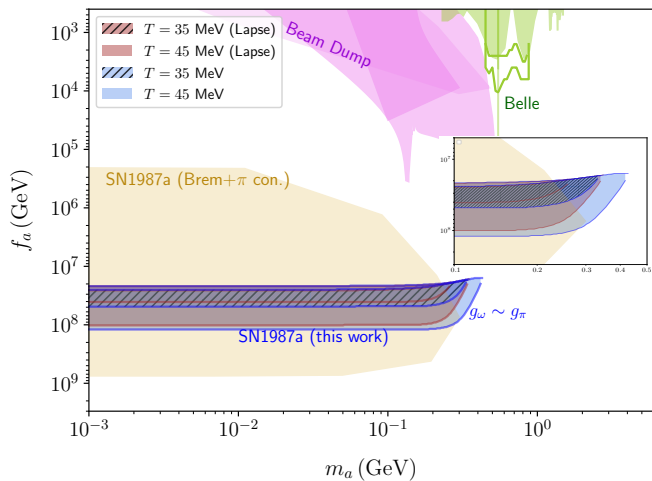


FIG. 4. Final exclusion plot due to the photo-production. The red and blue region corresponds to limits from the emissivity from photo-production processes. The blue region is devoid of any lapse correction while the red region takes it into account with ($\alpha = 0.84$). For all curves, we considered a KSVZ axion model with $C_A \approx 0.2$. Exclusion limits from beam dump experiments [14–16], rare decays of K [23, 27] and B -mesons [28–30] are shown in magenta and green respectively. We recast the previous bounds [75] on axion parameter space from bremsstrahlung and pion conversion in yellow. Limits on effective axion-photon coupling $g_{a\gamma\gamma}$ [79, 80], from HB stars [81, 82], CAST [83], Sumico [80] and light shining through wall [84] are important but not relevant for our region of interest.

F. Emitted Spectrum

The emissivity is related to the number density of particles emitted via

$$Q_a = \int dE_a E_a \frac{d^2 n_a}{dE_a dt}, \quad (22)$$

where the spectrum is defined as the number of axions emitted per interval of energy and time. Comparing with Eq. (10), it is straightforward to obtain the spectrum in the ND limit and for $m_a \ll T$. Furthermore, the total emitted flux is well approximated by integrating the spectrum over the radius of the star in the optically thin limit. Taking $R_{\text{PNS}} \approx 10$ Km, we obtain, in the range $E_a \in [0, 145]$

$$\begin{aligned} \frac{d^2 N_a^{\text{WZW}}}{dE_a dt} &\approx C_f^{\text{WZW}} \rho_{15} \left(\frac{C_A 10^9}{f_a/\text{GeV}} \right)^2 g_{10}^4 \left(\frac{E_a}{\text{MeV}} \right)^6 e^{-E_a/T}, \\ C_f^{\text{WZW}} &= 1.8 \times 10^{40} \text{ MeV}^{-1} \text{ s}^{-1}, \end{aligned} \quad (23)$$

and in the range $E_a \in [145, \infty]$,

$$\begin{aligned} \frac{d^2 N_a^{\text{data}}}{dE_a dt} &\approx C_f^{\text{data}} \rho_{15} \left(\frac{C_A 10^9}{f_a/\text{GeV}} \right)^2 \frac{\sigma_{\gamma n \rightarrow n\pi_0}^{\text{data}}}{\mu b} \left(\frac{E_a}{\text{MeV}} \right)^2 e^{-E_a/T} \\ C_f^{\text{data}} &\approx 8.4 \times 10^{48} \text{ MeV}^{-1} \text{ s}^{-1}. \end{aligned} \quad (24)$$

As shown in Fig. 5 by the blue curve, the total flux from the WZW photo-production is distinctively different from axion bremsstrahlung, with a comparatively harder spectrum.

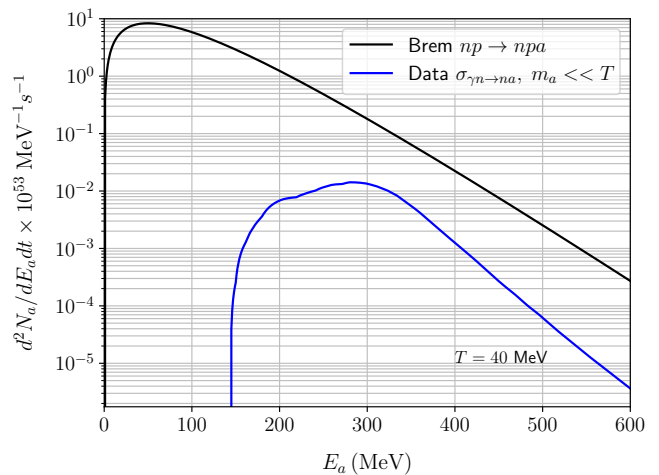


FIG. 5. Spectrum of axions due to WZW photo-production (blue) and bremsstrahlung [89] (black). We observe that the number of axions from photo-production is always at least one order of magnitude below the contribution from bremsstrahlung.

G. Axion detection prospects

Finally, we discuss the prospect of detecting such axions in Water Cerenkov experiments [39] such as Hyper-Kamiokande with fiducial mass 374 ktons [90]. Usually, axions emitted during future galactic SN can interact with the detector via the channels $ap \rightarrow p\gamma$ and $ap \rightarrow n\pi^+$ [50]. Around the peak of the WZW axion spectrum, i.e., $E_a \sim 200 - 300$ MeV, the cross-section for $ap \rightarrow n\pi^+$ is dominated by the $\Delta(1.23 \text{ GeV})$ resonance and roughly translates to $\sigma_{ap \rightarrow N\pi^+} \approx 10^{-25} C_A^2 (f_\pi/f_a)^2 \text{ cm}^{-2}$ [91]. Assuming N_t target particles, we evaluated the number of pions produced during such interaction can be obtained:

$$\begin{aligned} \frac{dN_\pi}{dt} &\approx 0.2 \rho_{15} C_A^4 \left(\frac{10^9}{f_a/\text{GeV}} \right)^4 \left(\frac{\text{Kpc}}{d} \right)^2 \\ &\times \left(\frac{M_{\text{detector}}}{\text{kton}} \right) \left(\frac{\text{g/mol}}{m_{H_2O}} \right), \end{aligned} \quad (25)$$

where $m_{H_2O} = 18 \text{ g/mol}$ the molecular mass of water. A SN at a distance of 0.2 Kpc with axions having $f_a = 10^9 \text{ GeV}$, would only roughly produce ~ 1 pion in the Hyper-Kamiokande, on a timescale of 10 seconds. This production is thus likely negligible.

III. SUMMARY & OUTLOOK

In summary, we study in detail the emissivity during supernovae originating from axion photo-production, i.e., $\gamma N \rightarrow Na$. We use the experimentally obtained scattering rates available in the range $E_\gamma \sim E_a \in [145, 500]$ MeV together with the contribution from the WZW term $\epsilon^{\mu\nu\alpha\beta} F_{\mu\nu} \partial_\alpha a \omega_\beta$. We find that photo-production is subdominant with respect to the usual axion bremsstrahlung process $NN \rightarrow NNa$, as depicted in Fig. 4 in most of the parameter space. It could however bring relevant corrections in the range of massive axions $m_a \gtrsim 100$ MeV, but we emphasize that such a claim would require further numerical computations [92]. Moreover, the spectrum of such axions is distinctively harder compared to the prototypical SN cooling processes, with a peak in the spectrum around $E_a \sim (5 - 6)T$.

Alternatively, photo-production of axions can also be probed at GlueX[93], where the photon beam of ~ 10 GeV hits a fixed target and produces a plethora of mesons. As far as degenerate neutron stars are concerned, we find that the cooling rate scales as T^9 and is subdominant compared to $NN \rightarrow NNa$.

ACKNOWLEDGEMENTS

SC thanks the Science and Engineering Research Board, Govt. of India (SRG/2023/001162) for financial support. MV is supported by the ‘‘Excellence of Science - EOS’’ - be.h project n.30820817, and by the Strategic Research Program High-Energy Physics of the Vrije Universiteit Brussel. AG is supported by the ‘‘Generalitat Valenciana’’ and CSIC through the GenT Excellence Program (CIDEIG/2022/22). MV thanks IFIC (Valencia) and CSIC for their hospitality during the completion of this project and Alberto Mariotti for comments on the draft. Authors would also like to thank Andrea Caputo, Stefan Stelzl, Konstantin Springmann and Michael Stadlbauer for very helpful discussions on the draft.

Appendix A: Wess-Zumino-Witten Interactions

The dynamics and interactions of Goldstone bosons associated with the spontaneous breaking of chiral symme-

try is aptly described by the Chiral Lagrangian (χ PT). At the leading order, the Lagrangian consists of terms

$$\mathcal{L} = \frac{f_\pi^2}{4} \text{Tr} (D_\mu U^\dagger D^\mu U + U^\dagger \chi + \chi^\dagger U) , \quad (\text{A1})$$

where $D_\mu U = \partial_\mu U - ir_\mu U + iU\ell_\mu$. r_μ and ℓ_μ describe left and right-handed currents which can be used to construct the vector and axial vector currents. Moreover, $\chi = 2B_0\mathcal{M}$, where χ is the isospin symmetry breaking spurion with \mathcal{M} denoting the quark mass matrix. Constants B_0 and f_π are fixed by experiments. However, Eq. (A1) possesses more symmetries such as spurious parity and charge conjugation compared to its underlying UV theory, i.e., QCD. As a result, χ PT in Eq. A1 fails to describe processes such as $K^+K^- \rightarrow \pi^+\pi^-\pi^0$ and $\pi^0 \rightarrow \gamma\gamma$, which are otherwise allowed in QCD. Such interactions can be restored in the Chiral Lagrangian by the Wess-Zumino-Witten term. In the geometric representation of the WZW form, one considers a 5-dimensional action, whose boundary is identified with 4-dimensional space in the form

$$S_{WZW}(U) = \kappa \int_D d^5y \omega , \text{ where} \\ \omega = -\frac{i}{240\pi^2} \epsilon^{\mu\nu\rho\sigma\tau} \text{Tr} [\mathcal{U}_\mu \mathcal{U}_\nu \mathcal{U}_\rho \mathcal{U}_\sigma \mathcal{U}_\tau] . \quad (\text{A2})$$

Here, we define $\mathcal{U}_\mu = U^\dagger \partial_\mu U$ and $\mathcal{U} \approx \text{Exp}(2i\pi^a T^a / f_\pi)$ with $f_\pi = 93$ MeV. Under chiral symmetry, U transforms as $U \rightarrow RUL^\dagger$ with R and L describing the $SU(2)_R$ and $SU(2)_L$ transformation matrices. Note that Eq. (A2) correctly describes the process $K^+K^- \rightarrow \pi^+\pi^-\pi^0$. To generate $\pi^0 \rightarrow \gamma\gamma$ or similar processes, one has to gauge S_{WZW} . However, any gauging has to be done in the 4-dimension. In principle, any arbitrary subgroup of the WZW action can be gauged and the resultant terms are

$$S_{WZW}(U, A_L, A_R) = S_{WZW}(U) \\ + \frac{N_c}{48\pi^2} \int d^4x \epsilon^{\mu\nu\rho\sigma} Z_{\mu\nu\rho\sigma} \quad (\text{A3})$$

where the full expression of $Z_{\mu\nu\rho\sigma}$ has been nicely tabulated in Ref. [52]. However, for our work, we only track the pion fields and therefore the relevant terms are

$$Z_{\mu\nu\rho\sigma}(U, A_L, A_R) \supset i \text{Tr} [\{ (\partial_\mu A_{\nu L}) A_{\rho L} + A_{\mu L} (\partial_\nu A_{\rho L}) \} \partial_\sigma U U^{-1} + \{ (\partial_\mu A_{\nu R}) A_{\rho R} + A_{\mu R} (\partial_\nu A_{\rho R}) \} U^{-1} \partial_\sigma U] \\ + i \text{Tr} [\{ (\partial_\mu A_{\nu R}) U^{-1} A_{\rho L} \partial_\sigma U + A_{\mu L} U^{-1} (\partial_\nu A_{\rho R}) \partial_\sigma U \}] . \quad (\text{A4})$$

Expanding in pion fields, $\partial_\mu U$ can be written as

$$\partial_\mu U = i \frac{\partial_\mu \pi_0}{f_\pi} \begin{pmatrix} 1 & 0 \\ 0 & -1 \end{pmatrix} + \dots \quad (\text{A5})$$

This choice results in a canonically normalized kinetic term from π_0 . Moreover, in the SM, the gauge fields are

expressed as

$$A_L = g_2 W^a \frac{\tau^a}{2} + g_1 W^0 \begin{pmatrix} \frac{1}{6} & 0 \\ 0 & \frac{1}{6} \end{pmatrix}, \quad (\text{A6})$$

$$A_R = g_1 W^0 \begin{pmatrix} \frac{2}{3} & 0 \\ 0 & -\frac{1}{3} \end{pmatrix}. \quad (\text{A7})$$

The physical gauge fields A and Z are introduced after electroweak symmetry breaking and they are related with W^0 and W^3 fields via the weak rotation angle θ_w as

$$W^0 = -s_W Z + c_W A, \quad W^3 = c_W Z + s_W A. \quad (\text{A8})$$

Using $g_1 c_W = g_2 s_W = e$, Eq. (A7) becomes

$$A_L = g_2 s_W \frac{A}{2} \begin{pmatrix} 1 & 0 \\ 0 & -1 \end{pmatrix} + g_1 c_W A \begin{pmatrix} \frac{1}{6} & 0 \\ 0 & \frac{1}{6} \end{pmatrix}, \quad (\text{A9})$$

$$= eA \begin{pmatrix} \frac{2}{3} & 0 \\ 0 & -\frac{1}{3} \end{pmatrix} = A_R. \quad (\text{A10})$$

To introduce the vector mesons fields, we use the background field method presented in Ref. [57] where $\tilde{A}_{L,R} = A_{L,R} + B_{L,R}$ (the charge as been included inside the definition of the field), including both the fundamental and background gauge fields. As a result, we make the following replacement $A_{L,R} \rightarrow \tilde{A}_{L,R}$ in Eq. (A4). The background field ω is then identified as

$$B_V = \frac{2g_\omega}{3} \omega \begin{pmatrix} 1 & 0 \\ 0 & 1 \end{pmatrix}, \quad B_A = 0, \quad (\text{A11})$$

$$\Rightarrow B_L = B_R = \frac{B_V}{2} = \frac{g_\omega}{3} \omega \begin{pmatrix} 1 & 0 \\ 0 & 1 \end{pmatrix}. \quad (\text{A12})$$

Using the definition of $A_{L,R}$ and $B_{L,R}$ as well as $N_c = 3$, fixed by matching with QCD, we find from Eq. (A4)

$$\begin{aligned} \mathcal{L}_{\text{WZW}} \supset & \frac{N_c}{24\pi^2} e g_\omega \frac{\partial_\rho \pi_0}{f_\pi} \epsilon^{\mu\nu\rho\sigma} F_{\mu\nu} \omega_\sigma \\ & + \frac{N_c}{96\pi^2} e^2 \epsilon^{\mu\nu\rho\sigma} \frac{\pi_0}{f_\pi} F_{\mu\nu} F_{\rho\sigma}. \end{aligned} \quad (\text{A13})$$

The coefficient $N_c = 3$ is fixed by matching with QCD.

Appendix B: Computation of the emissivities for the axion

In this section, we present the computation of the emissivities of the WZW photo-production reaction $\gamma N \rightarrow Na$ for the non-degenerate case and then for the degenerate case.

1. Emissivity in the non-degenerate case

We study the $2 \rightarrow 2$ interaction $\gamma N \rightarrow Na$ in the non-degenerate limit. In the centre of mass frame of the

collision, $E_{CM} = E_{N_1} + E_\gamma = E_{N_2} + E_a$. The matrix element takes the form

$$\langle |\mathcal{M}|^2 \rangle = 8 \frac{\kappa^2 m_N^2 g_\omega^2}{f_a^2 m_\omega^4} \left(E_\gamma^2 |\vec{p}_a|^2 \sin^2 \theta \right) + \mathcal{O}(p_F^2/m_N^2), \quad (\text{B1})$$

with $\kappa \equiv C_A g_\omega e N_c / 24\pi^2$. We also neglect m_γ compared to the energy scale. θ is the angle between the incoming neutron and the outgoing axion and p_F is the Fermi momentum of neutrons. Also, E_i and \vec{p}_i are the energy and three-momenta of the i^{th} species. In the CM frame $E_{CM} \equiv E_{N_1} + E_\gamma = E_{N_2} + E_a$, $E_\gamma \approx E_a$ and $E_a^2 = p_a^2 + m_a^2$. The cross-section for the $N\gamma \rightarrow Na$ process is given by

$$\begin{aligned} \frac{d\sigma_{N\gamma \rightarrow Na}}{d\Omega} &= \frac{|\vec{p}_a|}{|\vec{p}_\gamma|} \frac{\langle |\mathcal{M}|^2 \rangle}{64\pi^2 E_{CM}^2} \theta(E_{cm} - m_N - m_a), \\ &\approx \frac{\sqrt{E_a^2 - m_a^2}}{E_\gamma} \frac{\langle |\mathcal{M}|^2 \rangle}{64\pi^2 m_N^2} \theta(E_{CM} - m_N - m_a). \end{aligned} \quad (\text{B2})$$

The emissivity rate in the non-degenerate limit is expressed as

$$\begin{aligned} Q_{\text{ND}}^{\gamma N \rightarrow Na} &\approx \int \frac{g_\gamma d^3 \vec{p}_\gamma}{(2\pi)^3} f_\gamma(p_\gamma) \int \frac{g_N d^3 \vec{p}_N}{(2\pi)^3} f_N \int \frac{\langle |\mathcal{M}|^2 \rangle}{4E_{N_1} E_\gamma} \\ &(2\pi)^4 \delta^4 \left(\sum_i p_i \right) \frac{d^3 \vec{p}_2 d^3 \vec{p}_a}{(2\pi)^6 4E_a E_{N_2}} E_a. \end{aligned} \quad (\text{B3})$$

which can be further simplified with

$$\begin{aligned} Q_{\text{ND}}^{\gamma N \rightarrow Na} &\approx \int \frac{g_\gamma d^3 \vec{p}_\gamma}{(2\pi)^3} f_\gamma(p_\gamma) \int \frac{g_N d^3 \vec{p}_N}{(2\pi)^3} f_N \sigma(E_\gamma) E_a, \\ \sigma(E_\gamma) &\approx \frac{1}{3\pi} \frac{\kappa^2 g_\omega^2}{f_a^2 m_\omega^4} \sqrt{1 - \frac{m_a^2}{E_\gamma^2}} E_\gamma^2 (E_\gamma^2 - m_a^2), \end{aligned} \quad (\text{B4})$$

where $\sigma(E_\gamma)$ is the integrated cross section. The nucleon density is given by

$$n_B \equiv \int \frac{d^3 p_N}{(2\pi)^3} g_N f_N, \quad n_B = 4.5 \times 10^6 \rho_{15} \text{ MeV}^3.$$

Plugging Eq.(B5) in the emissivity Eq.(B4), we obtain

$$Q_{\text{ND}}^{N\gamma \rightarrow Na} \approx \frac{g_\gamma n_B}{3\pi} \frac{\kappa^2 g_\omega^2}{f_a^2 m_\omega^4} \int_{m_a}^{\infty} \frac{dE_\gamma}{2\pi^2} f_\gamma(p_\gamma) E_\gamma^7 (1 - m_a^2/E_\gamma^2)^{3/2}. \quad (\text{B5})$$

The two limiting conditions are:

1. $m_a/T \rightarrow 0$: In the limit $m_a/T \rightarrow 0$, we can approximate $\sqrt{1 - \frac{m_a^2}{E_\gamma^2}} \rightarrow 1$. This results in

$$Q_{\text{ND}}^{N\gamma \rightarrow Na} \approx \frac{g_\gamma n_B}{3\pi^3} \frac{4\pi^8}{15} \frac{\kappa^2 g_\omega^2}{f_a^2 m_\omega^4} T^8 \approx 27 g_\gamma n_B \frac{\kappa^2 g_\omega^2}{f_a^2 m_\omega^4} T^8. \quad (\text{B6})$$

Using the values and the normalization of the parameters explained in the main text along with $g_\gamma = 2$, we get

$$\frac{Q_{\gamma N \rightarrow Na}^{\text{WZW,ND}}}{10^{32} \text{ erg/s/cm}^3} \approx 2.2 g_{10}^4 T_{40}^8 \rho_{15} \left(\frac{C_A 10^9}{f_a/\text{GeV}} \right)^2. \quad (\text{B7})$$

2. $m_a/T \gtrsim 1$: In the opposite limit $m_a/T \gtrsim 1$, the mass of the axion cannot be neglected anymore and the expression becomes

$$\frac{Q_{\text{ND}}^{N\gamma \rightarrow Na}}{4 \times 10^{28} \text{ erg/s/cm}^3} \approx \left(\frac{C_A m_N 10^9}{f_a} \right)^2 g_{10}^4 \times \rho_{15} G(m_a, T_{40}), \quad (\text{B8})$$

where we defined the G function in terms of the Bessel functions as

$$G(m_a, T) \equiv 3m_a^4 T^2 \left(4m_a T K_3 \left(\frac{m_a}{T} \right) + (m_a^2 + 35T^2) K_4 \left(\frac{m_a}{T} \right) \right). \quad (\text{B9})$$

$$S(q^\mu) \equiv g_{N_1} \int \frac{d^3 \vec{p}_{N_1} d^3 \vec{p}_{N_2} m_N^2}{(2\pi)^6 E_{N_1} E_{N_2}} f_N(E_{N_1}) (1 - f_N(E_{N_2})) \times (2\pi)^4 \times \delta(E_{N_1} + Q_0 - E_{N_2}) \delta^3(\vec{p}_{N_1} - \vec{p}_{N_2} + \vec{q}) \Theta(E_{N_1} - m_N) \Theta(E_{N_2} - m_N), \quad (\text{B11})$$

and can be computed while identifying $z = Q_0/T$ and $|\vec{q}| \equiv q$. We obtain the final form of the response function

$$S(Q_0, q) = \frac{M_N^2 Q_0}{\pi q} \frac{1}{1 - e^{-z}} \Theta(\mu - E_-). \quad (\text{B12})$$

$$E^- = \sqrt{\left(m_N + \frac{Q_0}{2} \right)^2 + \left(\frac{\sqrt{q^2 - Q_0^2}}{2} - \frac{m_N Q_0}{\sqrt{q^2 - Q_0^2}} \right)^2} - \left(m_N + \frac{Q_0}{2} \right). \quad (\text{B13})$$

which can be simplified further

$$E^- \approx \sqrt{m_N^2 + \left(\frac{m_N Q_0}{\sqrt{q^2 - Q_0^2}} \right)^2} - m_N. \quad (\text{B14})$$

To perform the integral over p_a , we make the following change of variables

$$qdq = E_a E_\gamma d \cos \theta, \quad dQ_0 = dE_a, \\ \rightarrow \int \frac{d^3 p_a}{(2\pi)^3 2E_a} = \int \frac{dQ_0 dq}{(2\pi)^2 2E_\gamma} \frac{1}{E_\gamma}, \quad (\text{B15})$$

2. Emissivity in the degenerate case

We now evaluate the emissivity in the presence of strongly degenerate neutrons. The full expression is provided in a convenient form as

$$Q_{\text{axion}}^{N\gamma \rightarrow Na} = 2 \frac{\kappa^2}{f_a^2} \int \frac{d^3 \vec{p}_\gamma}{(2\pi)^3} g_\gamma \frac{f_\gamma}{2E_\gamma} \int \frac{d^3 \vec{p}_a}{(2\pi)^3 2E_a} \\ \times \left[2E_\gamma E_a (p_\gamma \cdot p_a) - (p_\gamma \cdot p_a)^2 \right] S(q^\mu) E_a. \quad (\text{B10})$$

where we define $Q_0 \equiv E_2 - E_1 = E_\gamma - E_a$, $\vec{q} = \vec{p}_\gamma - \vec{p}_a$. The response function is defined as

and the integral becomes

$$Q_{\text{D}}^{N\gamma \rightarrow Na} = \frac{g_\gamma \kappa^2}{f_a^2} \int \frac{d^3 p_\gamma}{(2\pi)^3} \frac{f_\gamma}{E_\gamma} \int \frac{dQ_0 dq}{(2\pi)^2 2E_\gamma} \frac{M_N^2 Q_0}{\pi} \\ \times \left[2E_\gamma E_a (p_\gamma \cdot p_a) - (p_\gamma \cdot p_a)^2 \right] \frac{E_\gamma - Q_0}{1 - e^{-Q_0/T}} \Theta(\mu - E_-). \quad (\text{B16})$$

The expression between the parenthesis in Eq.(B16) can be rewritten

$$\left[2E_\gamma E_a (p_\gamma \cdot p_a) - (p_\gamma \cdot p_a)^2 \right] = \left[(E_\gamma E_a)^2 - (\vec{p}_\gamma \cdot \vec{p}_a)^2 \right] \\ \approx \frac{(q^2 - Q_0^2)}{4} \left(-(q^2 - Q_0^2) + 4E_\gamma (E_\gamma - Q_0) \right). \quad (\text{B17})$$

To perform the integral, we need to define the boundaries of integration. Kinematics impose the condition that q variable varies from $q \in [Q_0, 2E_\gamma - Q_0]$. The Theta function in Eq.(B16) combined with the expression for E_- in Eq.(B14) further impose the lower bound on the q region of integration as $b|Q_0|$. In the end, we

get

$$q \in \left[b|Q_0|, 2E_\gamma - Q_0 \right], \quad a \equiv (\mu_N/M_N + 1)^2 - 1, \\ b \equiv \sqrt{\frac{a+1}{a}}. \quad (\text{B18})$$

Taking the typical value $\mu_N = 300$ MeV, we find $b \approx 1.56$. We will use those two values as a range of uncertainty for the degenerate density of the proto-NS. This induces that the Q_0 integral should be performed between

$$Q_0 \in \left[-\frac{2}{b-1}E_\gamma, \frac{2}{b+1}E_\gamma \right]. \quad (\text{B19})$$

We can further separate the parameter space into the region of

$$Q_0 \in \left[-\frac{2}{b-1}E_\gamma, 0 \right], \quad Q_0 \in \left[0, \frac{2}{b+1}E_\gamma \right]. \quad (\text{B20})$$

The integral over q can be trivially performed and by finishing the integration numerically, we obtain

$$\frac{Q_{\gamma N \rightarrow Na}^{\text{WZW,D}}}{10^{32} \text{erg/s/cm}^3} \approx 0.66 g_{10}^4 T_{40}^9 \left(\frac{C_A 10^9}{f_a/\text{GeV}} \right)^2. \quad (\text{B21})$$

Appendix C: Sources of uncertainty of WZW emissivity

In this subsection, we briefly discuss the main sources of uncertainty associated with the WZW photo-emission of axions. As we will see and as we foresaw in the main text, this essentially comes from the uncertainty on the values of nuclear physics quantities in an extremely dense medium like a SN and the uncertainty on the value of g_ω . We conclude that the uncertainty from the coupling largely dominates the final uncertainty on the emissivity.

1. In medium uncertainties

The Brown-Rho scaling dictates that the variation of the mass of the vector mesons follows the neutron mass[94]:

$$\frac{f_\pi^*}{f_\pi} \approx \frac{m_\omega^*}{m_\omega} \approx \frac{m_N^*}{m_N} \Rightarrow \frac{g_\omega^*}{g_\omega} \approx \frac{g_\pi^*}{g_\pi} \approx \frac{g_A^*}{g_A}. \quad (\text{C1})$$

where the \star indicates that the quantity is evaluated in the dense environment of the NS [41, 71, 89]. The m_N dependence is obtained from [89, 95]. For the g_A dependence, we use two different scaling laws: thick line from [41, 96] and dashed line from [97, 98], $g_A^*/g_A \approx 1/(1+(1/3)(m_N^*/m_N)(\rho/\rho_0)^{1/3})$. In the case of the axion bremsstrahlung, such effects led to only moderate uncertainties in the coupling [41, 99]. For $\rho/\rho_0 \in [0.5, 1]$, the uncertainties in the WZW photo production amounts to

$$\frac{Q_{N\gamma \rightarrow Na}^*}{Q_{N\gamma \rightarrow Na}} \approx \frac{m_\omega^4 g_{\omega^*}^4}{g_\omega^4 m_{\omega^*}^4} \in [0.8, 1.5]. \quad (\text{C2})$$

We conclude that the uncertainty on the emissivity from the in-medium effect is very mild.

We however emphasize that the in-medium corrections to the data-driven approach will not scale in this simple way and can receive large corrections.

2. The value of g_ω

As we discussed in the main text, one of the main sources of uncertainty of our work comes from the value of the coupling g_ω itself, since the emissivity scales like g_ω^4 and thus the bound on f_a scales like g_ω^2 . To alleviate this uncertainty on the coupling, we adopted a data-driven approach in all the regions where data for the pion-photo-production was available. We then fitted the cross-section and applied the mixing angle to obtain a cross-section for the axion photo-production. In Fig. 1 we present the data points used and our fit.

-
- [1] R. D. Peccei and H. R. Quinn, Phys. Rev. Lett. **38**, 1440 (1977).
 - [2] R. D. Peccei and H. R. Quinn, Phys. Rev. D **16**, 1791 (1977).
 - [3] S. Weinberg, Phys. Rev. Lett. **40**, 223 (1978).
 - [4] F. Wilczek, Phys. Rev. Lett. **40**, 279 (1978).
 - [5] G. 't Hooft, Phys. Rev. Lett. **37**, 8 (1976).
 - [6] J. Preskill, M. B. Wise, and F. Wilczek, Phys. Lett. B **120**, 127 (1983).
 - [7] M. Dine and W. Fischler, Phys. Lett. B **120**, 137 (1983).
 - [8] L. F. Abbott and P. Sikivie, Phys. Lett. B **120**, 133 (1983).
 - [9] P. W. Graham, D. E. Kaplan, and S. Rajendran, Phys. Rev. Lett. **115**, 221801 (2015), arXiv:1504.07551 [hep-ph].
 - [10] A. Hook and G. Marques-Tavares, JHEP **12**, 101 (2016), arXiv:1607.01786 [hep-ph].
 - [11] S. Trifinopoulos and M. Vanvlasselaer, Phys. Rev. D **107**, L071701 (2023), arXiv:2210.13484 [hep-ph].
 - [12] R. T. Co and K. Harigaya, Phys. Rev. Lett. **124**, 111602 (2020), arXiv:1910.02080 [hep-ph].
 - [13] S. Chakraborty, T. H. Jung, and T. Okui, Phys. Rev. D **105**, 015024 (2022), arXiv:2108.04293 [hep-ph].
 - [14] J. D. Bjorken, S. Ecklund, W. R. Nelson, A. Abashian, C. Church, B. Lu, L. W. Mo, T. A. Nunamaker, and P. Rassmann, Phys. Rev. D **38**, 3375 (1988).
 - [15] J. Blumlein *et al.*, Z. Phys. C **51**, 341 (1991).
 - [16] F. Bergsma *et al.* (CHARM), Phys. Lett. B **157**, 458 (1985).
 - [17] A. Aguilar-Arevalo *et al.* (PIENU), Phys. Lett. B **798**, 134980 (2019), arXiv:1904.03269 [hep-ex].

- [18] D. Pocanic *et al.*, Phys. Rev. Lett. **93**, 181803 (2004), arXiv:hep-ex/0312030.
- [19] W. Altmannshofer, S. Gori, and D. J. Robinson, Phys. Rev. D **101**, 075002 (2020), arXiv:1909.00005 [hep-ph].
- [20] H. Georgi, D. B. Kaplan, and L. Randall, Phys. Lett. B **169**, 73 (1986).
- [21] W. A. Bardeen, R. D. Peccei, and T. Yanagida, Nucl. Phys. B **279**, 401 (1987).
- [22] D. S. M. Alves and N. Weiner, JHEP **07**, 092 (2018), arXiv:1710.03764 [hep-ph].
- [23] S. Gori, G. Perez, and K. Tobioka, JHEP **08**, 110 (2020), arXiv:2005.05170 [hep-ph].
- [24] A. V. Artamonov *et al.* (E949), Phys. Lett. B **623**, 192 (2005), arXiv:hep-ex/0505069.
- [25] C. Lazzeroni *et al.* (NA62), Phys. Lett. B **732**, 65 (2014), arXiv:1402.4334 [hep-ex].
- [26] J. K. Ahn *et al.* (KOTO), Phys. Rev. Lett. **122**, 021802 (2019), arXiv:1810.09655 [hep-ex].
- [27] M. Bauer, M. Neubert, S. Renner, M. Schnubel, and A. Thamm, Phys. Rev. Lett. **127**, 081803 (2021), arXiv:2102.13112 [hep-ph].
- [28] D. Aloni, Y. Soreq, and M. Williams, Phys. Rev. Lett. **123**, 031803 (2019), arXiv:1811.03474 [hep-ph].
- [29] S. Chakraborty, M. Kraus, V. Loladze, T. Okui, and K. Tobioka, Phys. Rev. D **104**, 055036 (2021), [Erratum: Phys.Rev.D 108, 039903 (2023)], arXiv:2102.04474 [hep-ph].
- [30] E. Bertholet, S. Chakraborty, V. Loladze, T. Okui, A. Soffer, and K. Tobioka, Phys. Rev. D **105**, L071701 (2022), arXiv:2108.10331 [hep-ph].
- [31] M. Bauer, M. Neubert, S. Renner, M. Schnubel, and A. Thamm, JHEP **09**, 056 (2022), arXiv:2110.10698 [hep-ph].
- [32] G. G. Raffelt, physrep **198**, 1 (1990).
- [33] G. G. Raffelt, *Stars as laboratories for fundamental physics: The astrophysics of neutrinos, axions, and other weakly interacting particles* (1996).
- [34] N. Iwamoto, Phys. Rev. Lett. **53**, 1198 (1984).
- [35] N. Iwamoto, Phys. Rev. D **64**, 043002 (2001).
- [36] C. Hanhart, D. R. Phillips, and S. Reddy, Phys. Lett. B **499**, 9 (2001), arXiv:astro-ph/0003445.
- [37] T. Fischer, S. Chakraborty, M. Giannotti, A. Mirizzi, A. Payez, and A. Ringwald, Phys. Rev. D **94**, 085012 (2016), arXiv:1605.08780 [astro-ph.HE].
- [38] A. Burrows, M. T. Ressel, and M. S. Turner, Phys. Rev. D **42**, 3297 (1990).
- [39] J. Engel, D. Seckel, and A. C. Hayes, Phys. Rev. Lett. **65**, 960 (1990).
- [40] W. Keil, H.-T. Janka, D. N. Schramm, G. Sigl, M. S. Turner, and J. Ellis, Phys. Rev. D **56**, 2419 (1997).
- [41] R. Mayle, J. R. Wilson, J. Ellis, K. A. Olive, D. N. Schramm, and G. Steigman, Physics Letters B **219**, 515 (1989).
- [42] M. S. Turner, H.-S. Kang, and G. Steigman, Phys. Rev. D **40**, 299 (1989).
- [43] S.-Y. Ho, J. Kim, P. Ko, and J.-h. Park, Phys. Rev. D **107**, 075002 (2023), arXiv:2212.01155 [hep-ph].
- [44] M. S. Turner, Phys. Rev. D **45**, 1066 (1992).
- [45] G. Raffelt and D. Seckel, Phys. Rev. D **52**, 1780 (1995).
- [46] P. Carena, B. Fore, M. Giannotti, A. Mirizzi, and S. Reddy, Phys. Rev. Lett. **126**, 071102 (2021).
- [47] K. Choi, H. J. Kim, H. Seong, and C. S. Shin, JHEP **02**, 143 (2022), arXiv:2110.01972 [hep-ph].
- [48] M. Cavan-Piton, D. Guadagnoli, M. Oertel, H. Seong, and L. Vittorio, (2024), arXiv:2401.10979 [hep-ph].
- [49] P. W. Graham and S. Rajendran, Phys. Rev. D **88**, 035023 (2013), arXiv:1306.6088 [hep-ph].
- [50] G. Lucente, L. Mastrototaro, P. Carena, L. Di Luzio, M. Giannotti, and A. Mirizzi, Phys. Rev. D **105**, 123020 (2022), arXiv:2203.15812 [hep-ph].
- [51] J. Wess and B. Zumino, Phys. Lett. B **37**, 95 (1971).
- [52] E. Witten, Nucl. Phys. B **223**, 422 (1983).
- [53] O. Kaymakcalan, S. Rajeev, and J. Schechter, Phys. Rev. D **30**, 594 (1984).
- [54] K.-c. Chou, H.-y. Guo, K. Wu, and X.-c. Song, Phys. Lett. B **134**, 67 (1984).
- [55] H. Kawai and S. H. H. Tye, Phys. Lett. B **140**, 403 (1984).
- [56] N. K. Pak and P. Rossi, Nucl. Phys. B **250**, 279 (1985).
- [57] J. A. Harvey, C. T. Hill, and R. J. Hill, Phys. Rev. D **77**, 085017 (2008), arXiv:0712.1230 [hep-th].
- [58] J. A. Harvey, C. T. Hill, and R. J. Hill, Phys. Rev. Lett. **99**, 261601 (2007), arXiv:0708.1281 [hep-ph].
- [59] C. T. Hill and R. J. Hill, Phys. Rev. D **76**, 115014 (2007), arXiv:0705.0697 [hep-ph].
- [60] S. Chakraborty, A. Gupta, and M. Vanvlasselaer, JCAP **10**, 030 (2023), arXiv:2306.15872 [hep-ph].
- [61] S. Chakraborty, A. Gupta, and M. Vanvlasselaer, Journal of Cosmology and Astroparticle Physics **2023**, 030 (2023).
- [62] Y. Bai and C. H. de Lima, (2023), arXiv:2311.18794 [hep-ph].
- [63] B. Strandberg *et al.*, Phys. Rev. C **101**, 035207 (2020), arXiv:1812.03023 [nucl-ex].
- [64] W. J. Briscoe, A. E. Kudryavtsev, I. I. Strakovsky, V. E. Tarasov, and R. L. Workman, Eur. Phys. J. A **56**, 218 (2020), arXiv:2004.01742 [nucl-th].
- [65] W. J. Briscoe *et al.* (A2), Phys. Rev. C **100**, 065205 (2019), arXiv:1908.02730 [nucl-ex].
- [66] D. Drechsel, S. S. Kamalov, and L. Tiator, Eur. Phys. J. A **34**, 69 (2007), arXiv:0710.0306 [nucl-th].
- [67] L. Di Luzio, M. Giannotti, E. Nardi, and L. Visinelli, Phys. Rept. **870**, 1 (2020), arXiv:2003.01100 [hep-ph].
- [68] A. Notari, F. Rompineve, and G. Villadoro, Phys. Rev. Lett. **131**, 011004 (2023), arXiv:2211.03799 [hep-ph].
- [69] G. Grilli di Cortona, E. Hardy, J. Pardo Vega, and G. Villadoro, JHEP **01**, 034 (2016), arXiv:1511.02867 [hep-ph].
- [70] P. Braccini, C. Bradaschia, R. Castaldi, L. Foà, K. Lübelmeyer, and D. Schmitz, Nuclear Physics B **24**, 173 (1970).
- [71] A. Payez, C. Evoli, T. Fischer, M. Giannotti, A. Mirizzi, and A. Ringwald, JCAP **02**, 006 (2015), arXiv:1410.3747 [astro-ph.HE].
- [72] W. J. Briscoe, M. Hadžimehmedović, A. E. Kudryavtsev, V. V. Kulikov, M. A. Martemianov, I. I. Strakovsky, A. Švarc, V. E. Tarasov, R. L. Workman, S. Abt, P. Achenbach, C. S. Akondi, F. Afzal, P. Aguar-Bartolomé, Z. Ahmed, J. R. M. Annand, H. J. Arends, K. Bantawa, M. Bashkanov, R. Beck, M. Biroth, N. Borisov, A. Braghieri, S. A. Bulychjov, F. Cividini, C. Collicott, S. Costanza, A. Denig, E. J. Downie, P. Drexler, S. Fegan, M. I. Ferretti Bondy, S. Gardner, D. Ghosal, D. I. Glazier, I. Gorodnov, W. Gradl, M. Günther, D. Gurevich, L. Heikenskjöld, D. Hornidge, G. M. Huber, A. Käser, V. L. Kashevarov, S. Kay, M. Korolija, B. Krusche, A. Lazarev, K. Livingston,

- S. Lutterer, I. J. D. MacGregor, R. Macrae, D. M. Manley, P. P. Martel, J. C. McGeorge, D. G. Middleton, R. Miskimen, E. Mornacchi, A. Mushkarenkov, C. Mullen, A. Neganov, A. Neiser, M. Ostrick, P. B. Otte, H. Osmanović, R. Omerović, B. Oussena, D. Paudyal, P. Pedroni, A. Powell, S. N. Prakhov, G. Ron, T. Rostomyan, A. Sarty, C. Sfienti, V. Sokhoyan, K. Spieker, J. Stahov, O. Steffen, I. Supek, A. Thiel, M. Thiel, A. Thomas, L. Tiator, M. Unverzagt, Y. A. Usov, N. K. Walford, D. P. Watts, S. Wagner, D. Werthmüller, J. Wettig, M. Wolfes, and N. Zachariou (A2 Collaboration at MAMI), *Phys. Rev. C* **100**, 065205 (2019).
- [73] P. Carena, T. Fischer, M. Giannotti, G. Guo, G. Martínez-Pinedo, and A. Mirizzi, *JCAP* **10**, 016 (2019), [Erratum: *JCAP* **05**, E01 (2020)], arXiv:1906.11844 [hep-ph].
- [74] A. Lella, P. Carena, G. Lucente, M. Giannotti, and A. Mirizzi, *Phys. Rev. D* **107**, 103017 (2023), arXiv:2211.13760 [hep-ph].
- [75] A. Lella, P. Carena, G. Co', G. Lucente, M. Giannotti, A. Mirizzi, and T. Rauscher, *Phys. Rev. D* **109**, 023001 (2024), arXiv:2306.01048 [hep-ph].
- [76] A. Caputo, H.-T. Janka, G. Raffelt, and E. Vitagliano, *Phys. Rev. Lett.* **128**, 221103 (2022), arXiv:2201.09890 [astro-ph.HE].
- [77] G. Lucente, P. Carena, T. Fischer, M. Giannotti, and A. Mirizzi, *JCAP* **12**, 008 (2020), arXiv:2008.04918 [hep-ph].
- [78] N. Iwamoto, *Phys. Rev. D* **64**, 043002 (2001).
- [79] P. Agrawal *et al.*, *Eur. Phys. J. C* **81**, 1015 (2021), arXiv:2102.12143 [hep-ph].
- [80] P. W. Graham, I. G. Irastorza, S. K. Lamoreaux, A. Lindner, and K. A. van Bibber, *Ann. Rev. Nucl. Part. Sci.* **65**, 485 (2015), arXiv:1602.00039 [hep-ex].
- [81] A. Ayala, I. Domínguez, M. Giannotti, A. Mirizzi, and O. Straniero, *Phys. Rev. Lett.* **113**, 191302 (2014), arXiv:1406.6053 [astro-ph.SR].
- [82] O. Straniero, A. Ayala, M. Giannotti, A. Mirizzi, and I. Dominguez, in *11th Patras Workshop on Axions, WIMPs and WISPs* (2015) pp. 77–81.
- [83] V. Anastassopoulos *et al.* (CAST), *Nature Phys.* **13**, 584 (2017), arXiv:1705.02290 [hep-ex].
- [84] J. Redondo and A. Ringwald, *Contemp. Phys.* **52**, 211 (2011), arXiv:1011.3741 [hep-ph].
- [85] J. E. Kim, *Phys. Rev. Lett.* **43**, 103 (1979).
- [86] M. A. Shifman, A. I. Vainshtein, and V. I. Zakharov, *Nucl. Phys. B* **166**, 493 (1980).
- [87] A. R. Zhitnitsky, *Sov. J. Nucl. Phys.* **31**, 260 (1980).
- [88] M. Dine, W. Fischler, and M. Srednicki, *Phys. Lett. B* **104**, 199 (1981).
- [89] G. G. Raffelt, *The Astrophysical Journal* **561**, 890 (2001).
- [90] K. Abe *et al.*, (2011), arXiv:1109.3262 [hep-ex].
- [91] E. M. Henley and A. Garcia, *Subatomic Physics: Third Edition* (2007).
- [92] S. Chakraborty, A. Gupta, and M. Vanvlasselaer, .
- [93] D. Aloni, C. Fanelli, Y. Soreq, and M. Williams, *Phys. Rev. Lett.* **123**, 071801 (2019), arXiv:1903.03586 [hep-ph].
- [94] G. E. Brown and M. Rho, *Phys. Rev. Lett.* **66**, 2720 (1991).
- [95] *nphysa* **473**, 760 (1987).
- [96] M. Rho, *Phys. Rev. Lett.* **54**, 767 (1985).
- [97] D. N. Voskresensky, *Lect. Notes Phys.* **578**, 467 (2001), arXiv:astro-ph/0101514.
- [98] T. Fischer, *Astron. Astrophys.* **593**, A103 (2016), arXiv:1608.05004 [astro-ph.HE].
- [99] R. Mayle, J. R. Wilson, J. Ellis, K. Olive, D. N. Schramm, and G. Steigman, *Physics Letters B* **203**, 188 (1988).